PHYSICAL REVIEW B VOLUME 25, NUMBER 2 15 JANUARY 1982

Defect energetics in α-Al_2O_3 and rutile TiO_2

C. R. A. Catlow and R. James
Department of Chemistry, University College London, 20 Gordon Street, London WC1H OAJ, United Kingdom

W. C. Mackrodt and R. F. Stewart
I. C. I. Corporate Laboratory, P. O. Box 11, The Heath, Runcorn, Cheshire WA7 4QE, United Kingdom

(Received 10 June 1980; revised manuscript received 16 March 1981)

We report a theoretical survey of defect energetics in α-Al_2O_3 and rutile TiO_2 which we relate to structural and transport properties of these materials. The study of these crystals has required us to modify our computational methods based on the Mott-Littleton theory, which were previously confined to the treatment of cubic materials. We discuss the theoretical aspects of a new and quite general computational procedure, HADES III, which can be used for defect calculations on crystals of any symmetry. Our discussion pays particular attention to the effects on the calculated energetics of the use of Mott-Littleton methods adapted for anisotropic crystals. Other features, considered in detail, are the sensitivity of calculated defect energies to the choice of lattice potential and to the size of the atomistically simulated region surrounding the defect. We also compare our results for α-Al_2O_3 and those of an earlier study of Dienes *et al.* Our calculations are then used to discuss the simplest features of the defect properties of pure and doped α-Al_2O_3 and TiO_2. The present results support the dominance of Schottky disorder in both crystals; cation Frenkel energies are high and anion Frenkel pairs may be of significance in α-Al_2O_3. In addition we present a survey of doped alumina and of the effect of oxygen partial pressure on the defect structure of this material. Our results suggest that defect clustering will have a major influence on the properties of doped Al_2O_3.

I. INTRODUCTION

In recent years there has been considerable success in the calculation of defect energies in ionic oxides using computational methods. Studies of UO_2 (Ref. 1) and the divalent transition oxides[2–4] have shown that methods based essentially on the original work of Mott and Littleton[5] can yield good quantitative agreement between calculated and experimental defect energies. Moreover, the methods can be applied to the investigation of the complex modes of defect aggregation in heavily defective phases (see, e.g., the study of Catlow and Fender[6] on $Fe_{1-x}O$).

The present study reports an extension of the computational methods to more complex structures than those which have hitherto been investigated. Our paper has therefore two main purposes: first, to report and discuss the modifications of technique that were necessary for the calculations on the noncubic crystals Al_3O_3 and TiO_2; second, to present our calculated energies for basic defects in the pure and doped oxides, which we relate to experimental data on the materials. Our study concentrates on Al_2O_3. The calculations on TiO_2 are used largely to illustrate the improvements following from the use of our modified Mott-Littleton code. A more detailed study of disorder in rutile will be presented elsewhere.[7]

Modification of the computational techniques is necessary as previous work has been confined to crystals with dielectric isotropy, that is to say, crystals of cubic symmetry. (That a crystal be cubic is a necessary but not a sufficient condition for the validity of the defect simulation methods used to date. Methods based on the model of dielectric isotropy are only strictly applicable to a crystal in which the point-group symmetry of all lattice sites

is cubic. Certain crystals where the *system* is cubic may not fulfill this criterion; an example is the perovskite structure where the anions are not at sites of cubic symmetry.) This restriction arises essentially from the structure of the computational techniques. These simulate the defective crystal by surrounding the defect with an inner atomistically treated region (region I) and an outer region (region II) in which ionic displacements and dipoles are calculated using simple formulas employing the macroscopic dielectric constant (see Mott and Littleton,[5] and for a general discussion, Lidiard and Norgett[8]). The calculations published to date treat the latter region isotropically—an approximation which is strictly valid only for cubic crystals.

A further restriction of most previous calculations concerns the lattice potential used in the treatment of the inner atomistic region. These potentials have been derived empirically by fitting to bulk crystal data—a procedure which should give a reliable lattice model for separations close to those observed for the perfect lattice but which for defective crystals, where the interatomic spacings may differ considerably, is more questionable.

In our study particular attention will be paid to the problems of the anisotropy of region II and of the lattice potentials. As remarked, the crystals are noncubic; the structures of both the corundum lattice of alumina and the rutile lattice adopted by TiO_2 are based on hexagonal close packing of the oxide sublattice. We have therefore developed a general computer code, HADES III, which can be used for defect calculations on noncubic crystals. The program supersedes the earlier HADES II package written by Norgett,[8,9,10] which was confined to cubic systems. The development of HADES III has necessitated not only the introduction of anisotropy in the treatment of region II as discussed above but also modification of the symmetry routines which previously had been specifically adapted for cubic systems. These points will be further discussed in Sec. II.

The role of crystal potentials in determining the reliability of the calculations is also an important theme of this paper. We will compare the results of calculations performed using empirical potentials of the type outlined above with those employing nonempirical potentials obtained from developments[3] of the electron-gas model of Wedepohl[11] and Gordon and Kim.[12,13] This section of our study will allow us to assess both the sensitivity of our results to the crystal potential as well as the reliability of the two ways of parametrizing lattice models.

Another feature determining the reliability of our calculations is the size of the atomistically simulated region. Earlier studies on cubic materials, e.g., CaF_2 (Ref. 14) and UO_2 (Ref. 1), found rapid monotonic convergence of the calculated defect energies to a constant value as the size of region I was increased. We find that the behavior of noncubic materials is significantly different. The convergence is slower; that is, larger sizes of the inner region I are needed before the calculated defect energies become roughly constant. In addition, the variation for noncubic crystals of the defect energy with region size is irregular, contrasting with the monotonic behavior generally observed for cubic systems. We will return to these points in Sec. IV.

In the case of Al_2O_3, earlier theoretical defect studies have been reported by Dienes *et al.*[15] These workers used methods broadly similar to those employed in this study, although there were significant differences in both technique and in the lattice potentials. Several of the results of their study are in fair agreement with our calculations, but in certain cases we do find large differences between the two sets of calculations. These will also be considered in Sec. IV.

The following two sections contain an account of the methods used in the defect calculations, paying particular attention to the extensions of technique necessary in the development of the completely general HADES III package. Section III contains a discussion of lattice potentials—both empirical and nonempirical. Section IV presents our results on basic defect energetics, and in Sec. V calculations on doped Al_2O_3 are discussed. The defect structure of doped TiO_2 is complicated by the possibility of deviations from the stoichiometric composition; this is planned to be discussed in a separate publication. Our discussion of the results will highlight two aspects of the theory of defect energetics: first, the comparison between the results obtained for noncubic crystals using isotropic and anisotropic approximations for the dielectric continuum; second, the comparison of calculations based on empirical and nonempirical potentials. Our results illustrate the necessity, in certain cases, for an accurate treatment of the dielectric anisotropy of noncubic systems; furthermore, the sensitivity of the calculated energies to the details of the individual potentials is found to be critical for some defects. Detailed comparison of our results with experiment is not possible at this stage partly in view of the complexity of the data. In addition, howev-

er, such a discussion requires that defect mobility be considered explicitly and calculations of this sort will form the basis of subsequent publications. General predictions of the defect and transport properties, however, are possible, and in addition, our calculations provide a guide as to the basic features of the defect structure of the doped oxides.

II. DEFECT CALCULATIONS

The defect calculations reported in this paper are based on the Mott-Littleton method[5] developed by Lidiard and Norgett[8] and Norgett[9,10] and implemented, for cubic materials, in the HADES computer package. For noncubic crystals, such as those considered here, while the fundamental theory for treating lattice defects remains the same, a number of important changes in the formulation are essential to allow for the anisotropy of the structures. Since an account of HADES methodology is not generally available, the elements of the theory will be outlined with an emphasis on the changes needed for noncubic systems.

Throughout we follow the formulation presented by Norgett.[9,10] Quite formally, the crystal surrounding a defect is divided into an inner region I, which is explicitly relaxed and an outer region II, which is treated by some suitable continuum approximation. The total energy of the system E can then be written as

$$E = E_1(\vec{x}) + E_2(\vec{x},\vec{\xi}) + E_3(\vec{\xi}) \tag{2.1}$$

in which $E_1(\vec{x})$ is the energy of the inner region, $E_3(\vec{\xi})$ the energy of the outer region and $E_2(\vec{x},\vec{\xi})$ the interaction energy of regions I and II. $\vec{x}$ are the independent coordinates describing the configuration of the inner region while $\vec{\xi}$ are the displacements in region II and are formally distinguished from $\vec{x}$. $E_3(\vec{\xi})$ is assumed to be a quadratic function of $\vec{\xi}$; thus

$$E_3(\vec{\xi}) = \tfrac{1}{2}\vec{\xi}\cdot\underline{A}\cdot\vec{\xi}\ , \tag{2.2}$$

which together with the equilibrium condition,

$$\frac{\partial E}{\partial \vec{\xi}} = \left.\frac{\partial E_2(\vec{x},\vec{\xi})}{\partial \vec{\xi}}\right|_{\vec{\xi}=\vec{\xi}_e} + \underline{A}\cdot\vec{\xi} \tag{2.3}$$

in which $\vec{\xi}_e$ are the equilibrium values for $\vec{\xi}$ corresponding to arbitrary values of $\vec{x}$, leads to an alternative form for the total energy E which is given by

$$E = E_1(\vec{x}) + E_2(\vec{x},\vec{\xi}_e) - \frac{1}{2}\left.\frac{\partial E_2(\vec{x},\vec{\xi})}{\partial \vec{\xi}}\right|_{\vec{\xi}=\vec{\xi}_e}\cdot\vec{\xi}_e\ . \tag{2.4}$$

The significance of this rearrangement is that by making certain assumptions about $\vec{\xi}_e$, E can be made independent of $E_3(\vec{\xi}_e)$, which formally extends to infinity. The revised expression involves summation only over pairs of ions in region I, together with the interaction of I and II, of which part can be made near local while the remainder can be given in some closed form.

Now the defect energy E can be determined either by direct minimization with respect to $\vec{x}$, the displacements in region I, i.e., by solving the equations $dE/d\vec{x}=0$, or by the requirement that the force on each ion is zero, $(\partial E/\partial\vec{x})_{\vec{\xi}=\text{const}}=0$. As pointed out by Norgett,[8] the former, though entirely consistent, is difficult to apply in view of the complicated nature of E as a function of $\vec{x}$. The "force-balance" requirement, on the other hand, is rather more straightforward and is equivalent to the direct minimization provided that the outer region is in equilibrium, i.e., $(\partial E/\partial\vec{\xi})_{\vec{x}}=0$, since

$$\frac{dE}{d\vec{x}} = \left.\frac{\partial E}{\partial\vec{x}}\right|_{\vec{\xi}} + \left.\frac{\partial E}{\partial\vec{\xi}}\right|_{\vec{x}}\cdot\frac{\partial\vec{\xi}_e}{\partial\vec{x}}\ . \tag{2.5}$$

The solution of the force-balance equations for ionic lattices has been discussed by Norgett and Fletcher[16] who have described a method based on the Fletcher-Powell variable-metric technique.[17] The appropriate optimization procedures are implemented in the HADES package and were used throughout for the present calculations. Clearly, E approaches the "true" defect energy as the size of region I is increased, though this, of course, increases the number of variables to be optimized and hence the computational time. Now it is a matter of experience that for convergence, the number of ions needed in region I is of the order of 10,[2] so that within a "shell-model" description of the system the total number of variables is $\sim 6\times 10^2$, which is clearly prohibitive. A major feature of the HADES formulation, then, is its maximal use of symmetry to reduce the number of working variables to within reasonable limits. To achieve this for the crystal structures reported here, the complete subgroup of 48 cubic symmetry operations was included in the symmetry processing of region I for TiO_2, whereas for Al_2O_3 the corresponding subgroup consisted of 36 hexagonal elements. The net result is that for the present calcu-

lations in excess of 10^2 ions could be included in the explicit region.

Turning now to an explicit two-body representation for E, the energy of the perfect lattice is written as

$$E_L = \sum_{i>j} \Phi_{ij}(|\vec{R}_i - \vec{R}_j|) \tag{2.6}$$

in which Φ_{ij} is some suitable pair potential and $\vec{R}$ the appropriate lattice coordinates. Likewise, the energy of the lattice containing the defect is given by

$$E_D = \sum_{i>j} \Phi_{ij}(|\vec{r}_i - \vec{r}_j|), \tag{2.7}$$

in which $\vec{r}$ are the displaced coordinates. The energy of the defect, therefore, is simply given by

$$E = \sum_{i>j} [\Phi_{ij}(|\vec{r}_i - \vec{r}_j|) - \Phi_{ij}(|\vec{R}_i - \vec{R}_j|)] . \tag{2.8}$$

Now the identification of Eq. (2.1) or its alternative form, Eq. (2.4), with Eq. (2.8) is not quite as straightforward a matter as it might seem. For while E_1 is evidently given by

$$E_1 = \sum_{\substack{i\in I \\ j\in I}} [\Phi_{ij}(|\vec{r}_i - \vec{r}_j|) - \Phi_{ij}(|\vec{R}_i - \vec{R}_j|)] , \tag{2.9}$$

a simple summation of the type $\sum_{i\in II, j\in II}$ for the outer region is not an adequate description of E_3 since it is not a quadratic function of the displacements $\vec{r}_i - \vec{R}_i$, as required by Eq. (2.2). Additional interactions need to be included to suppress the linear dependence on the displacement which arises from the power-series expansion of $\Phi_{ij}(|\vec{r}_i - \vec{r}_j|) - \Phi_{ij}(|\vec{R}_i - \vec{R}_j|)$ in region II. After some manipulation it can be shown that the correct expression for E_3 is

$$E_3 = \sum_{\substack{i\in II \\ j\in II}} [\Phi_{ij}(|\vec{r}_i - \vec{r}_j|) - \Phi_{ij}(|\vec{R}_i - \vec{R}_j|)] + \sum_{\substack{i\in I \\ j\in II}} [\Phi_{ij}(|\vec{R}_i - \vec{r}_j|) - \Phi_{ij}(|\vec{R}_i - \vec{R}_j|)] \tag{2.10}$$

It contains a contribution, therefore, which corresponds to a displaced region II with all the ions in region I at their perfect lattice sites without defects. E_2, then, is given by

$$E_2 = \sum_{\substack{i\in I \\ j\in II}} [\Phi_{ij}(|\vec{r}_i - \vec{r}_j|) - \Phi_{ij}(|\vec{R}_i - \vec{r}_j|)] , \tag{2.11}$$

so that the final expression for E is

$$E = \sum_{\substack{i\in I \\ j\in I}} [\Phi_{ij}(|\vec{r}_i - \vec{r}_j|) - \Phi_{ij}(|\vec{R}_i - \vec{R}_j|)] + \sum_{\substack{i\in I \\ j\in II}} [\Phi_{ij}(|\vec{r}_i - \vec{r}_j|) - \Phi_{ij}(|\vec{R}_i - \vec{r}_j|)] - \tfrac{1}{2} \sum_{\substack{i\in I \\ j\in II}} \left[\frac{\partial}{\partial \vec{r}_j} \Phi_{ij}(|\vec{r}_i - \vec{r}_j|) - \frac{\partial}{\partial \vec{r}_j} \Phi_{ij}(|\vec{R}_i - \vec{r}_j|) \right] \cdot (\vec{r}_j - \vec{R}_j) . \tag{2.12}$$

Equations (2.6)–(2.12) are perfectly general and apply to systems of all types. For ionic crystals the situation in general is complicated because of the long-range nature of the Coulomb interaction. This can be eased, however, by fully exploiting the natural separation of interatomic potentials into short- and long-range contributions, and is achieved by use of the Ewald method for calculating the Madelung terms, wherein the nominal long-range interaction is transformed to summations over direct and reciprocal lattices. The former, being manifestly local in nature, can be evaluated together with the repulsive terms and so lead to considerable computational simplications.

The interactions in region I are purely local and can be dealt with *exactly* for crystals of arbitrary structure. In the outer region, on the other hand, there is a contribution from long-range interactions which by necessity requires analytic evaluation. In the neighborhood of region I, the interaction between I and II comprises both long- and short-range terms which can be dealt with by direct summation. Away from the boundary between the two regions the interaction is purely Coulombic and the corresponding energy E_2' can be shown to reduce to the form

$$E_2' = \sum_{\substack{i\in I \\ j\in II'}} q_i q_j \left[\frac{1}{|\vec{r}_i - \vec{r}_j|} - \frac{1}{|\vec{r}_i - \vec{R}_j|} - \frac{1}{|\vec{R}_i - \vec{r}_j|} + \frac{1}{|\vec{R}_i - \vec{R}_j|} \right] , \tag{2.13}$$

which can be written as

$$E_2' = \sum_{\substack{i \text{ over all} \\ \text{vacancies in I} \\ j\in \text{II}'}} q_i q_j \left[-\frac{1}{|\vec{R}_i - \vec{r}_j|} + \frac{1}{|\vec{R}_i - \vec{R}_j|} \right] + \sum_{\substack{i \text{ over all} \\ \text{interstitials in I} \\ j\in \text{II}'}} q_i q_j \left[\frac{1}{|\vec{r}_i - \vec{r}_j|} - \frac{1}{|\vec{r}_i - \vec{R}_j|} \right]$$

$$+ \sum_{\substack{i \text{ over all} \\ \text{lattice ions in I} \\ j\in \text{II}'}} q_i q_j \left[\frac{1}{|\vec{r}_i - \vec{r}_j|} - \frac{1}{|\vec{r}_i - \vec{R}_j|} - \frac{1}{|\vec{R}_i - \vec{r}_j|} + \frac{1}{|\vec{R}_i - \vec{R}_j|} \right] . \tag{2.14}$$

Now it can be shown that the last summation, i.e., over lattice ions in region I, reduces to

$$\sum_{\substack{i \text{ over all} \\ \text{lattice ions in I} \\ j\in \text{II}'}} q_i q_j \left[\frac{\vec{\xi}_i \cdot \vec{\xi}_j}{|\vec{R}_i - \vec{R}_j|^3} - 3\frac{[\vec{\xi}_i \cdot (\vec{R}_i - \vec{R}_j)][\vec{\xi}_j \cdot (\vec{R}_i - \vec{R}_j)]}{|\vec{R}_i - \vec{R}_j|^5} \right] + \cdots \tag{2.15}$$

in which $\vec{\xi}_i = \vec{r}_i - \vec{R}_i$, and furthermore, that the leading term of the corresponding summation in E_3' is of exactly the same form. These are simply the interaction of displacement dipoles in region I with the corresponding dipoles in region II, and for sufficiently large region I, are assumed to be negligible. E_2' and E_3', *therefore, are given solely by the interaction of vacancies and interstitials with the outermost parts of region II.* Without loss of generality, the individual defects can *separately* be considered as being located at the origin of the coordinate system, so that E_2' reduces to

$$E_2' = Q \sum_{j\in \text{II}'} q_j \left[-\frac{1}{|\vec{r}_j|} + \frac{1}{|\vec{R}_j|} \right] \tag{2.16}$$

in which Q is the *total* "effective" charge of the defect. (N.B. that for vacancies, q_i is minus the corresponding ionic charge.) Writing the displacement $\vec{\xi}_j$ as $\vec{r}_j - \vec{R}_j$, Eq. (2.16) can now be expanded to give

$$E_2' = -Q \sum_{j\in \text{II}'} q_j \left[\frac{\vec{\xi}_j \cdot \vec{R}_j}{|\vec{R}_j|^3} + \frac{1}{2}\frac{|\vec{\xi}_j|^2}{|\vec{R}_j|^3} - \frac{3}{2}\frac{(\vec{\xi}_j \cdot \vec{R}_j)^2}{|\vec{R}_j|^5} - \frac{3}{2}\frac{|\vec{\xi}_j|^2 (\vec{\xi}_j \cdot \vec{R}_j)}{|\vec{R}_j|^5} - \frac{3}{8}\frac{|\vec{\xi}_j|^4}{|\vec{R}_j|^5} + \cdots \right] \tag{2.17}$$

which for most cases of practical interest, viz., large $\vec{R}_j$, can be approximated by the leading term

$$E_2' = -Q \sum_{j\in \text{II}'} \frac{q_j (\vec{\xi}_j \cdot \vec{R}_j)}{|\vec{R}_j|^3} . \tag{2.18}$$

The total contribution from the outer part of region II, then is given by,

$$E_2' - \frac{1}{2}\frac{\partial E_2'}{\partial \vec{\xi}}\bigg|_{\vec{\xi} = \vec{\xi}_e} \cdot \vec{\xi}_e = -\tfrac{1}{2} Q \sum_{j\in \text{II}'} \frac{q_i (\vec{\xi}_{ej} \cdot \vec{R}_j)}{|\vec{R}_j|^3} \tag{2.19}$$

in which $\vec{\xi}_e$ are the equilibrium displacements.

Provided that the inner region is sufficiently large, then, the displacement of ions in the outer region is determined to all intents and purposes by the electric field due to effective charge of the defect(s), and an essential feature of the HADES methodology is the use of the Mott-Littleton approximation[5] to calculate these displacements. For a crystal containing s ions per unit cell, at zero bulk strain the change in the lattice energy ΔE in an external electric field $\vec{F}$ is given by

$$\Delta E = \tfrac{1}{2} \delta\vec{r}^T \cdot \underline{W} \cdot \delta\vec{r} - (\vec{q}^T \cdot \delta\vec{r})^\alpha F^\alpha \tag{2.20}$$

in which $\delta\vec{r}$ is a $3s$-dimensional vector of displacements, $\vec{q}$ an s-dimensional vector of ion charges and $\underline{W}$ a $(3s \times 3s)$ matrix,

$$\underline{W}^{\alpha\beta} = \frac{\partial^2 U_L}{\partial \vec{r}^\alpha \partial \vec{r}^\beta} \tag{2.21}$$

in which U_L is the field-free equilibrium lattice energy. At equilibrium in the presence of a field F, $\partial(\Delta E)/\partial(\delta\vec{r}) = 0$, so that

$$\delta\vec{r}^\alpha = ([\underline{W}^{-1}]^{\alpha\beta} \cdot \vec{q}) F^\beta . \tag{2.22}$$

From the definition of the electric displacement field $\vec{D}$ and the dielectric constant $\underline{K}$,

$$D^\alpha = F^\alpha + 4\pi P^\alpha \tag{2.23a}$$

$$= F^\alpha + \frac{4\pi}{v_c}(\vec{q}^{\,T}\cdot\delta\vec{r}^{\,\alpha}) \tag{2.23b}$$

$$= \left[\delta^{\alpha\beta} + \frac{4\pi}{v_c}(\vec{q}^{\,T}\cdot[\underline{W}^{-1}]^{\alpha\beta}\cdot\vec{q}\right] F^\beta \tag{2.23c}$$

$$= K^{\alpha\beta}F^\beta , \tag{2.23d}$$

thus

$$K^{\alpha\beta} = \left[\delta^{\alpha\beta} + \frac{4\pi}{v_c}(\vec{q}^{\,T}\cdot[\underline{W}^{-1}]^{\alpha\beta}\cdot\vec{q})\right] . \tag{2.24}$$

In Eqs. (2.23a)–(2.24) P^α is the polarization in the α direction, v_c the volume of the unit cell, and $\delta^{\alpha\beta}$ the Kroneker delta. The displacements $\delta\vec{r}$, therefore, are given by

$$\delta\vec{r}^{\,\alpha} = ([\underline{W}^{-1}]^{\alpha\beta}\cdot\vec{q})[\underline{K}^{-1}]^{\beta\gamma}D^\gamma . \tag{2.25}$$

For cubic materials, the ionic displacements are isotropic and reduce to the simple Mott-Littleton form,

$$\delta\vec{x} = \frac{v_c}{4\pi}\frac{([\underline{G}^{-1}]\cdot\vec{q})(1-\epsilon^{-1})}{(\vec{q}^{\,T}\cdot\underline{G}^{-1}\cdot\vec{q})}D^x \tag{2.26}$$

in which $\delta\vec{x}$ is an s-dimensional vector of displacements in *either* the x, y, or z directions, D^x the corresponding electric displacement, $\underline{G}$ the second derivative of the $(s\times s)$ non-Coulombic interaction matrix, and ϵ the trace of the dielectric constant tensor.

For defects with an effective charge Q, the dielectric displacement field at a distance R is given by

$$\vec{D} = -\frac{QR}{|\vec{R}|^3} \tag{2.27}$$

from which the ion displacements in region II′ and the interaction energy can be evaluated. For cubic materials the latter reduces to

$$E_2' + E_3' = -\tfrac{1}{2}Q^2\sum_{j\in II'} q_j\frac{m_j}{|\vec{R}_j|^4} , \tag{2.28}$$

where m_j is determined from Eq. (2.26), whereas for noncubic materials, it takes the more general form

$$E_2' + E_3' = -\tfrac{1}{2}Q^2\sum_{j\in II'}\left[\left(\sum_{\alpha\beta}M_j^{\alpha\beta}R_j^\alpha R_j^\beta\right)\Big/|\vec{R}_j|^6\right] \tag{2.29}$$

in which

$$M_j^{\alpha\beta} = ([\underline{W}^{-1}]^{\alpha\gamma}\cdot\vec{q})_j[\underline{K}^{-1}]^{\gamma\beta} . \tag{2.30}$$

Incomplete lattice sums of the type given in Eqs. (2.28) and (2.29) are evaluated by calculating the *complete* lattice sums analytically[18] and subtracting the explicit sums for the inner region.

In summary, then, the formal procedure for determining the defect energy E involves the evaluation of the displacements $\vec{\zeta}_e$ for the outer region and the solution of the "force-balance" equations $\partial E/\partial\vec{x}=0$ for constant $\vec{\zeta}_e$. For an explicit pairwise interaction, E_1 is simply given by Eq. (2.9), whereas the definition of E_3 requires some manipulation to reduce it to a quadratic function of the displacements. Both the local energy of region I and the interaction with the innermost part of region II are calculated explicitly, but the interaction with the outermost part of the crystal is reduced to a charge-induced dipole interaction involving *solely* the defects. The Mott-Littleton approximation is used to calculate the displacements in region II, which for simple cubic materials are isotropic and lead to an R^{-4} interaction. For noncubic materials, on the other hand, the displacements are anisotropic and the interaction energy is of the form $\sum_{\alpha\beta}M^{\alpha\beta}R^\alpha R^\beta/R^6$; one of the objectives of this work is to examine the influence of these anisotropic effects.

III. INTERIONIC POTENTIALS

Here, as elsewhere in the calculation of defect energies[14,2–4,15] we assume potentials that are essentially ionic and exclusively two body. To allow for electronic polarization of the lattice we use a simple shell model of the type introduced by Dick and Overhauser[19] in their treatment of the dielectric properties of the alkali halides and subsequently used by numerous authors.[14,2–4,15] Non-Coulombic interactions are assumed to operate solely between the shells, so that ions are subject to distortion by both short-range forces and electric polarization by the remainder of the lattice. These effects are of comparable magnitude and often oppose each other, so that there is a close relationship between the pair potentials of a crystal and the polarization of its constitutent ions.

Two approximate methods have been used for determining potentials, both of which have previously been described in some detail.[20] The first of these represents the non-Coulombic contribution to each pair potential as

TABLE I. Fitted potential parameters and shell constants for α-Al_2O_3 and TiO_2. In all cases the metal-metal pair potential is taken to be purely Coulombic.

Parameter or system	α-Al_2O_3	TiO_2
$A(+-)$ (eV)	1460.3	656.74
$\rho(+-)$ (Å)	0.29912	0.40431
$C_6(+-)$ (eV Å^6)	0.0	0.0
$A(--)$ (eV)	22764.3	22764.3
$\rho(--)$ (Å)	0.1490	0.1490
$C_6(--)$ (eV Å^6)	27.879	27.063
Y_+ ($\lvert\vec{e}\rvert$)	1.3830	−35.863
k_+ (eV Å^{-2})	92.488	65974.0
Y_- ($\lvert\vec{e}\rvert$)	−2.81061	−2.38856
K_- (eV Å^{-2})	103.07	18.413

$$V(r)_{\text{non-Coul}}=A\exp(-r/\rho)-C/r^6 \qquad (3.1)$$

in which r is the separation between the corresponding shells. The sets of parameters A, ρ, and C together with the appropriate shell constants Y and K are then obtained from an optimum fit to known lattice properties such as the cohesive energy, lattice parameters, and dielectric and elastic constants. For the most part this procedure has been confined to cubic materials, though it has recently been applied to MgF_2 and MnF_2 by Catlow, James, and Norgett[21] and Catlow and James.[22] A particular difficulty arises for noncubic materials in that potentials derived in this way can often lead to quite sizable bulk and internal strains in the lattice, which can seriously complicate the subsequent evaluation of accurate defect energies. In the present paper, therefore, we included a simultaneous minimization of the lattice strains in the fitting procedure for the various parameters. In Table I we list the relevant parameters and shell constants for α-Al_2O_3 and rutile TiO_2, while in

TABLE II. Calculated and observed crystal properties for Al_2O_3 and TiO_2.

Lattice properties or system	α-Al_2O_3		TiO_2	
	Calculated[a]	Observed	Calculated[a]	Observed
Lattice energy (eV)	−160.21	−160.4[b]	−109.90	126.0[b]
C_{11} (10^{11} dyn/cm^2)	42.96	49.69[c]	25.33	27.01[f]
C_{12}	15.48	16.36	17.80	17.66
C_{13}	12.72	11.09	20.90	14.80
C_{33}	50.23	49.8	77.92	48.19
C_{14}	−2.99	−2.35		
C_{44}	16.16	14.74	9.22	12.39
C_{66}	13.70	$(C_{11}-C_{12})/2$	22.12	19.30
ϵ_{11}^0	9.38	9.34[d]	94.76	86
ϵ_{33}^0	11.52	11.54[d]	157.32	170
ϵ_{11}^∞	2.08	3.1[e]	6.28	6.83
ϵ_{33}^∞	2.02		7.99	8.43

[a]Based on empirical potentials.
[b]Samsonov, Ref. 23.
[c]Elastic constants for this material taken from Wachtman *et al.*, Ref. 24.
[d]Young and Frederikse, Ref. 25.
[e]Levine, Ref. 26.
[f]Elastic and dielectric constants for TiO_2 taken from Traylor *et al.*, Ref. 27.

Table II we give the calculated cohesive energies and dielectric and elastic constants that derive from the corresponding potentials.

The second method we used for obtaining interionic potentials is that suggested by Mackrodt and Stewart[3] and used in a recent examination of the alkaline-earth oxides.[4] It is based on a modified form of the electron-gas approximation[11-13] in which cation densities, and in particular those for ions in high oxidation states, are assumed to be the free-ion values, while anion densities are derived from suitable atomic Hartree-Fock calculations which include a contribution from the Madelung potential for the crystal in question. Keeton and Wilson[28] and Dienes *et al.*[15] have adopted a related approach in their calculations on CaF_2 and α-Al_2O_3, respectively, but without the self-energy correction to the exchange energy derived by Rae.[29] A particularly useful feature of the electron-gas approximation is that interaction potentials involved in both redox reactions and doping, for example, can be calculated in exactly the same way as those for the host lattice, and here we use this procedure for the hole and electron states in α-Al_2O_3 and the oxide doped by Mg^{2+} and Ti^{4+}, as well as for the calculation of the basic defect energies. Details of all these potentials are given in Ref. 30. As yet there is no reliable, nonempirical procedure for obtaining shell constants, so these were found by fitting to the high frequency and static dielectric constants. We assume Al^{3+} to be nonpolarizable, and obtain the following values for oxygen: $Y_- = -1.974\,|\vec{e}\,|$ and $K_- = 16.0$ eV Å^{-2}. In Table III we list the calculated lattice properties for Al_2O_3 based on the electron-gas approximation, together with the experimental values.

The development of the two sets of potentials allows us to test the sensitivity of our results to potential parameters. This point will be discussed in the following section.

IV. BASIC DEFECT ENERGIES—RESULTS AND DISCUSSION

In this section we present first our calculated energies for vacancy and interstitial formation in Al_2O_3 and TiO_2, paying special attention to the effect on these results of the treatment of region II and of the choice of lattice potential. (The vacancy formation energy is that required to remove a lattice ion to infinity allowing the remaining lattice to relax to equilibrium. Likewise, the formation energy of an interstitial is that involved in bringing an ion from infinity to an interstitial site with a corresponding relaxation of the surrounding lattice.) Second, we discuss the problem of the convergence of calculated defect energies with expansion of region I, taking the cation vacancy and interstitial in Al_2O_3 as typical examples. In doing so we consider the way in which cubic and noncubic materials may differ in this respect. A comparison of our results with those previously reported by Dienes *et al.*[15] is considered next. Finally we consider the relation of our results to experiment.

A. Defect energetics

In Table III we present the results of a series of calculations on vacancies and interstitials (both cation and anion) in Al_2O_3 and TiO_2. We give values for both isotropic and anisotropic treatments of region II, and, in the case of Al_2O_3, for empirical and nonempirical potentials. For this material we also quote the results of the previous study of Dienes *et al.*[15] The results are then combined to give Frenkel and Schottky energies which are also reported as the energy per defect (i.e., the Frenkel-pair energy divided by two, and the energy of the Schottky quintet in Al_2O_3 divided by five). We also include the energy associated with interstitial disorder, i.e., $Al_2O_3 \rightleftarrows 2Al_I^{3+} + 3O_I^{2-}$. Calculations of the Schottky and interstitial disorder energies require the lattice cohesive energies, which are given in Tables II and III.

Perhaps the most striking feature of the results is the failure of the calculations on TiO_2 employing an isotropic region II to converge. The effect on region I of using an incorrect, isotropic field for the outer region is so severe as to lead to divergence. This must occur because an isotropic field due to the region-II displacements, when acting on the ions in region I, causes the latter to enter regions where the lattice model is unstable. The particular type of divergence encountered is a "polarization catastrophe" which involves the development of massive ionic dipoles during the iterative course of the caclulation. Shell-model potentials are usually less susceptible to this particular instability than simple point-dipole models (see Faux and Lidiard[31]); nevertheless, there are, in general, interatomic spacings at which the potentials are unstable, and it is clear that the calculations using the isotropic treatment of region I have led to relaxations which result in such spacings. Our study

TABLE III. Defect energies in (a) Al_2O_3 and (b) TiO_2. Values in parentheses are energies per defect.

(a) Al_2O_3

Defect	Calculated energies (eV)			
	Empirical potential calculations		Nonempirical potential calculations	
	Isotropic region II (HADES II)[b]	Anisotropic region II (HADES III)[c]	Anisotropic region II (HADES III)[c]	Previous study of Dienes *et al.*[a]
Anion interstitial	−16.34	−16.59	−5.22	−10.1
Anion vacancy	24.45	24.17	21.75	24.1
Cation vacancy	55.35	54.30	61.15	54.3
Cation interstitial	−42.42	−43.87	−46.98	−34.4
Cohesive energy	−160.53	−160.21	−161.85	−156.7
Schottky quintet energy	23.50 (4.70)	20.90 (4.18)	25.70 (5.14)	28.5 (5.7)
Anion Frenkel-pair energy	8.12 (4.06)	7.58 (3.79)	16.54 (8.27)	14.0 (7.0)
Cation Frenkel-pair energy	12.94 (6.47)	10.44 (5.22)	14.18 (7.09)	20.0 (10.0)
Interstitial disorder energy	26.67 (5.33)	22.70 (4.54)	52.23 (10.44)	57.6 (11.5)

(b) TiO_2

Defect	Calculated energies (eV) employing empirical potentials[d]
Anion interstitial	−8.58
Anion vacancy	17.30
Cation vacancy	80.58
Cation interstitial	−68.63
Schottky trio	5.22(1.84)
Anion Frenkel pair	8.72(4.36)
Cation Frenkel pair	11.96(5.98)

[a]The calculations of Dienes *et al.* (Ref. 15) used 30 ions in region I.
[b]HADES II calculations used 70 ions in region I.
[c]HADES III calculations used 80 ions in region I.
[d]HADES III calculations (HADES II failed to converge).

has therefore shown that the use of the incorrect region-II field for highly anisotropic materials can have a severe effect on the interaction between the two regions which may prevent the calculation from converging.

We note that TiO_2 indeed represents a particularly extreme case of dielectric anisotropy ($\epsilon_2=86$, $\epsilon_{11}=170$). In contrast, the dielectric properties of Al_2O_3 are largely isotropic ($\epsilon_{11}=\epsilon_{22}=9.34$, $\epsilon_{33}=11.54$). Thus the results in Table III(b) show relative insensitivity of the calculated defect energies for this material to the treatment of region II. The conclusion to be drawn from these comparisons is simple. Isotropic treatments of the continuum region in Mott-Littleton calculations for noncubic materials may be acceptable in the limited

number of cases where the dielectric properties are in fact nearly isotropic. When, however, there is significant anisotropy, the correct anisotropic treatment of the displacements, as incorporated in the HADES III package, is *essential* for reliable results. The highly anisotropic material TiO_2 provides an extreme example wherein an incorrect isotropic approximation leads to a divergence of the calculation.

The second comparative theme stressed in this paper concerns the effect of different potentials on our calculated energies. The calculated Schottky and Frenkel energies for Al_2O_3, as well as the individual defect energies in Table III(a), show reasonable agreement in all cases but that of the anion interstitial (and consequently the anion Frenkel energy) in Al_2O_3. The latter value is $\sim 3-4$ eV higher for the calculations using the nonempirical models. The energy of the O^{2-} ion in the interstitial site in Al_2O_3 is clearly sensitive to the parameters describing the $O^{2-} \cdots O^{2-}$ short-range potential, which differs very considerably for the two types of model. We should note the contrast between this behavior and that found for UO_2, where the large interstitial site results in relative insensitivity of the results to the choice of potential. In oxides with a close-packed anion sublattice (which is the case in Al_2O_3 and TiO_2 but not in UO_2) interstitial energies are clearly much more sensitive to potential parameters.

B. Convergence of calculations on noncubic crystals

In Table IV we present the results of calculations on the anion interstitial in Al_2O_3 as a function of the size of the inner, explicitly relaxed region. Three observations can be made on these results which are typical of the behavior of the calculated energies of isolated defects. First, the variation of the defect energy with the size of the inner region may be irregular; this contrasts with the smoother convergence observed by, for example, Catlow[1] for expansion of the inner region for defects in UO_2. Second, the defect energies do not converge to a constant value; once region I becomes sufficiently large the values vary irregularly with no tendency for a general decrease in energy with increase of the size of the region. These irregular variations are ~ 0.1 eV in magnitude, and they represent the limits of the accuracy of our calculated absolute energies. Similar behavior is found for cubic crystals, although the magnitude of this "noise" is smaller. Third, the convergence appears to be slower than in the cubic systems, e.g., UO_2. In the latter case, little variation of most defect energies (apart from the irregular "noise" just discussed) is observed after expansion of the inner region beyond ~ 60 ions. For the defects in Al_2O_3 appreciable variation is still observed for expansion beyond 100 ions.

TABLE IV. Anion interstitial energies as a function of size of region I.

Number of ions in region I	Calculated energy (eV)
21	−4.006
33	−4.053
45	−4.655
65	−5.203
71	−5.229
83	−5.218
101	−5.162
125	−5.201
149	−5.262
161	−5.343
185	−5.425

The superior convergence properties of calculations on cubic crystals is directly attributable to their higher symmetry. Owing to the isotropy of cubic materials spherical inner regions are clearly suitable. On the other hand, the anisotropy of noncubic systems would suggest that nonspherical inner regions are, perhaps, more appropriate; however, this refinement has not been implemented in the present calculations.

Thus for noncubic systems, particular care must be taken in discussing the results of defect calculations, especially in those cases where we are concerned with comparisons of energies (for example, in obtaining activation energies) where we must use comparable sizes of region I. Where absolute energies are important large sizes of region I should if possible be used to ensure that satisfactory approach to convergence has been achieved. The sizes of region I employed for the calculations reported in Table IV should be adequate for the accuracy required in the present study.

C. Comparison with previous theory

Dienes *et al.*[15] have reported a shell-model Mott-Littleton study of defect energies in Al_2O_3. Their approach, therefore, is basically similar to

that used in this paper. The potentials were somewhat different than those used here, although the short range parameters were derived using electron-gas methods of a type similar (though not identical) to those discussed in Sec. III. Two features of these previous calculations, however, suggest a lower order of reliability by comparison with the present work: first, the use of an isotropic treatment of the lattice displacement in region II; second, the small size (30 ions) of the explicitly relaxed inner region. The defect energies obtained by Dienes *et al.*[15] are given in Table III(a) together with our results. As seen, for vacancies of both types, the agreement is good; for interstitials, on the other hand, much larger differences are found. The latter may, in part, arise from differences in potentials, and in particular we believe that the cation-anion short-range potential used by these authors is probably too repulsive, thereby leading to a cation interstitial energy that is too high. Their anion interstitial energy is closer to our work and falls between the values derived from the two different potentials used in the present study.

This completes our review of the results on the basic defect energetics of Al_2O_3 and TiO_2. Questions of technique have been stressed in this section. We consider the comparison of our results with experiment in Sec. VI after we have discussed our calculations on doped Al_2O_3.

V. IMPURITY IONS IN Al_2O_3

The principal impurities in this material are tetravalent and divalent cations. Both types of dopant are considered in this section. We examine their modes of solution in the alumina host under two types of conditions: First, the divalent or tetravalent oxide enters the host without exchange of oxygen with the atmosphere; second, we consider the case when solutions of the impurity may be accompanied by oxygen loss or gain from the crystal.

The first section of our discussion will ignore the effect of defect interactions; the results here are therefore appropriate for systems at high dilution. We then present calculations on defect aggregation which allow us to discuss the behavior of crystals at higher dopant concentrations. The calculations on hole and electron states, necessary for our discussion of redox processes, also enable us to comment on the band structure of the solid; we summarize these results in the final part of this section. We concentrate on the Ti^{4+} and Mg^{2+} impurity ions. Other species are, however, also considered. These results enable us to discuss briefly the variation of the enthalpy of solution with the radius of the dopant ion.

The calculated energies of lattice and impurity defects needed for our survey in this section are presented in Table V(a). All were obtained using the nonempirical potentials, which for the impurity-lattice interactions were generated by the procedure discussed in Sec. III. For the substitutionals, values are reported only for Mg^{2+} and Ti^{4+}. Potentials are, however, available for the other dopant ions whose heats of solution are discussed in Sec. V A 3.

In calculating the energies of electron and hole states the simplest procedure is to assume a small polaron model for the hole, in which case calculations are performed for holes localized on a single oxide ion (i.e., an O^- ion). By analogy with vacancy and interstitial defects, the formation energy of the small polaron involves the removal of a lattice O^{2-} ion to infinity, its ionization to O^-, and subsequent return to the lattice allowing for relaxation of the surrounding ions. The use of such models simplifies the treatment of the hole species, whose energy may be estimated once the appropriate potentials for the interaction between lattice ions and the O^- species have been generated. These potentials were again obtained by the nonempirical procedures discussed in Sec. III. To obtain the hole formation energies we need to add to the lattice energy term calculated by HADES, the value of the electron affinity of the O^- ion. Colbourn and Mackrodt[32] have considered this and other aspects of the electronic structure of α-Al_2O_3 in some detail, and in this paper we use their values for the energy of conduction-band electrons and the hole formation energy. Details of these are given in Tables V(b) and VIII.

A simpler procedure may be used for the calculations required for our survey of hole-dopant clustering when this involves localization of a hole on a neighboring lattice site. No inclusion of electron affinity terms is necessary as we are only interested in the difference between hole energies at various sites in the crystal. In this context, the short-range potentials for the O^- ion may be treated as identical to the lattice oxide ion. Adjustment of the short-range potential does not significantly affect the binding energies which are mainly Coulombic in origin. This latter result was confirmed by detailed calculations on selected clusters.

TABLE V. Component energies for investigation of modes of solution of Mg^{2+} and Ti^{4+} solution in Al_2O_3. (a) Dopant and lattice defect energies; (b) hole and electron energies.

(a) Dopant and lattice defect energies (eV)

Lattice energy of MgO	−40.74
Lattice energy of TiO_2	−122.40
Lattice energy of Al_2O_3	−161.85
Al^{3+} interstitial energy	−46.98
Mg^{2+} interstitial energy	−16.20
Al^{3+} vacancy energy	−61.15
O^{2-} vacancy energy	−21.75
O^{2-} interstitial energy	−5.22
Mg^{2+} substitutional energy	32.46
Ti^{4+} substitutional energy	−31.31
Ti^{3+} substitutional energy	7.98

(b) Hole and electron energies (eV)

Lattice-energy term for hole formation	16.10
Effective ionization of O^{2-} in α-Al_2O_3	−8.4(32)
Hole formation energy	−7.7(32)
Measured band gap	9.5(33)
Conduction-band edge	−1.0(34)

We are now in a position to use our calculated energies to discuss modes of solution of the dopant ions. We assume throughout that these can be predicted on energetic ground alone, that is we neglect the contribution to the free energy of solution of vibrational defect entropies.

A. Crystals at high dilution: defect interactions omitted

1. *Solutions without exchange of oxygen with the atmosphere*

a. Tetravalent ions

The large Madelung potential at the cation site ensures that these species enter as cation substitutionals. We are concerned, therefore, with the nature of the charge compensation. There are two alternatives—cation vacancies or anion interstitials. In the former case, solution takes place with displacement by the tetravalent impurity of lattice cations to the surface with the creation of one cation vacancy for every three substitutionals. (The displaced cations are again removed to the surface.) The energy E_M^V per substitutional of this reaction may be written as

$$E_M^V = -E(MO_2) + \tfrac{2}{3}E(Al_2O_3) + E(M_{Al}^{4+}) + \tfrac{1}{3}E(V_{Al}) , \quad (5.1)$$

where $E(MO_2)$ is the lattice energy of the tetravalent oxide, $E(Al_2O_3)$ that of Al_2O_3, $E(M_{Al}^{4+})$ the energy of the tetravalent substitutional, and $E(V_{Al})$ the cation vacancy formation energy.

Equation (5.1) may be readjusted by noting that the Schottky energy per defect E_{Sch}^1 may be written as

$$E_{Sch}^1 = \tfrac{1}{5}[2E(V_{Al}) + 3E(V_O) + E(Al_2O_3)] ,$$

where $E(V_O)$ is the energy of the anion vacancy. We then write Eq. (5.1) as

$$E_M^V = -E(MO_2) + E(M_{Al}^{4+}) + \tfrac{1}{2}E(Al_2O_3) - \tfrac{1}{2}E(V_O) + \tfrac{5}{6}E_{Sch}^1 . \quad (5.2)$$

For the energy of the anion interstitial mode of compensation we have

$$E_M^I = -E(MO_2) + E(M_{AL}^{4+}) + \tfrac{1}{2}E(Al_2O_3) + \tfrac{1}{2}E(O_I) , \quad (5.3)$$

where $E(O_I)$ is the energy of the oxygen interstitial. Noting that the oxygen Frenkel energy per defect E_{OF}^1 is given by

$$E_{OF}^1 = \tfrac{1}{2}E(O_I) + \tfrac{1}{2}E(V_O) ,$$

we can write E_M^I as

$$E_M^I = -E(MO_2) + E(M_{Al}^{4+}) + \tfrac{1}{2}E(Al_2O_3) - \tfrac{1}{2}E(V_O) + E_{OF}^1 . \quad (5.4)$$

Comparing Eq. (5.2) with Eq. (5.4) we conclude that vacancy rather than interstitial compensation will operate if

$$\tfrac{5}{6}E_{Sch}^1 < E_{OF}^1 .$$

Results calculated using the empirical potentials suggest that $\frac{5}{6}E_{Sch}^1 \approx E_{OF}^1$. From these results, we can, therefore, draw no definite conclusion as to the nature of the charge compensation. If these calculations are correct, the nature of the predominant defects will probably be determined by the degree of stabilization that derives from clustering. However, if the results derived from nonempirical potentials are correct there is no question that cation vacancy compensation will dominate, as the Schottky energy per defect is considerably less than that of the oxygen Frenkel energy.

b. Divalent ions

As commented earlier, we concentrate here on the commonest divalent impurity in Al_2O_3, namely Mg^{2+}. Several modes of solution are possible for this species: First, the ion can dissolve *substitutionally* with either anion vacancy or cation interstitial compensation. Second, "self-compensating" modes of solution are possible in which Mg^{2+} substitutionals are charge compensated by Mg^{2+} interstitials. Third, the Mg^{2+} may dissolve entirely as *interstitials* with either cation vacancy or oxygen interstitial compensation. We may develop the following expressions for the enthalpy of solution, E_{Mg} of MgO in Al_2O_3 for the modes described above.

(i) Substitutional solutions. For the *vacancy* compensation we have the expression

$$E_{Mg}^V = -E(MgO) + E(Mg_{Al}^{2+}) + \tfrac{1}{2}E(V_O) + \tfrac{1}{2}E(Al_2O_3) , \quad (5.5)$$

where $E(Mg_{Al}^{2+})$ is the energy of the cation substitutional Mg^{2+} ion (with respect to Mg^{2+} and Al^{3+} ions at infinity). Other terms are as defined above. Aluminum interstitial compensation of the substitutional Mg^{2+} will result in an energy of solution given by

$$E_{Mg}^I = -E(MgO) + E(Mg_{Al}^{2+}) + \tfrac{1}{3}E(Al_I^{3+}) + \tfrac{1}{3}E(Al_2O_3) , \quad (5.6)$$

where $E(Al_I^{3+})$ is the energy of the aluminum interstitial ion.

(ii) Self-compensating solutions. Here, E_{Mg} is given by

$$E_{Mg}^S = -E(MgO) + \tfrac{2}{3}E(Mg_{Al}^{2+}) + \tfrac{1}{3}E(Mg_I^{2+}) + \tfrac{1}{3}E(Al_2O_3) , \quad (5.7)$$

where $E(Mg_I^{2+})$ is the formation energy of a Mg^{2+} interstitial with respect to ions at infinity.

(iii) Interstitial solution of Mg^{2+}. First we consider cation vacancy compensation for which we have the expression

$$E_{Mg} = -E(MgO) + E(Mg_I^{2+}) + \tfrac{2}{3}E(V_{Al}) + \tfrac{1}{3}E(Al_2O_3) , \quad (5.8)$$

where $E(V_{Al})$ is the energy of a cation vacancy. The alternative of oxygen interstitial compensation gives

$$E_{Mg} = -E(MgO) + E(Mg_I^{2+}) + E(O_I^{2-}) . \quad (5.9)$$

The energies calculated for the different modes of solution are given in Table VI. As noted earlier all the calculated quantities are derived from the modified electron-gas potentials. Similar qualitative conclusions follow the results based on the empirical potentials, though the details are not presented here. The results suggest that either the substitutional and/or vacancy or self-compensating modes of solution will dominate. If we bear in mind the sensitivity of our calculations, both seem equally favorable on energetic grounds. Furthermore, the energy for aluminum interstitial compensation of the Mg^{2+} substitutional is sufficiently high to allow this mode of solution to be eliminated for Mg^{2+}-doped Al_2O_3. A variety of charge-compensating modes would, therefore, seem to be possible in this defect solution, and the nature of the dominant defect is likely to be determined by the extent to which the different compensating defects are stabilized by the clustering which is discussed in Sec. V B. This situation exactly parallels that found by Mackrodt and Stewart[4] in their examination of the reduction of CdO in which defect aggregation was shown to play a critical role.

TABLE VI. Calculated enthalpies of solution (eV) of (a) MgO and (b) TiO_2 in α-Al_2O_3 at infinite dilution. Energies quoted per dissolved impurity ion. All values obtained using energies in Table I and expressions given in Sec. V A 1 of text.

(a) MgO	
Substitutional-vacancy mode	3.15
Self-compensating mode	3.03
Interstitial aluminum compensation	3.59
Interstitial Mg^{2+} with vacancy compensation	5.78
Interstitial Mg^{2+} with oxygen interstitial compensation	13.77
(b) TiO_2	
Substitutional-vacancy mode	3.53
Interstitial oxygen compensation	7.52

2. *Variation of solution energies with dopant ionic radius*

In this section we briefly summarize the results of a survey of the heats of solution of a variety of divalent and tetravalent oxides in Al_2O_3. For the divalent ions we considered substitutional solutions with anion vacancy compensation, while for the tetravalent ions, cation vacancy compensation was assumed. These substitutional energies were obtained from calculations which employed dopant-lattice interactions obtained using the electron-gas methods.[3,4] We report, however, in Table VII only the resulting heats of solution obtained using the expressions derived in the preceding section. Our calculated values are displayed graphically in Figs. 1 and 2.

TABLE VII. Calculated heats of solution ΔH_{sol} of aliovalent oxides in Al_2O_3 for (a) divalent and (b) tetravalent oxides.

Oxide	ΔH_{sol} (eV)
(a) Divalent oxides	
BeO	4.0
MgO	3.2(3.9)[a]
CaO	6.8
SrO	10.4
BaO	14.2
(b) Tetravalent oxides	
TiO_2[b]	3.5
SnO_2[b]	5.5
PbO_2[c]	7.1
ThO_2[c]	10.3

[a]Experiment data of Roy and Coble (Ref. 35).
[b]Rutile-structured oxide.
[c]Fluorite-structured oxide.

The results show that the heats of solution ΔH_{sol} of all oxides are high and positive, suggesting that the levels of impurities in solid solution in Al_2O_3 will be low even at high temperatures. The lowest energies are found for MgO and TiO_2—a result which is clearly compatible with the observation of these ions as the major impurity species in alumina. For the tetravalent dopant, we find the expected monotonic increase of the heat of solution with the radius of the tetravalent ion. For the divalent ions a minimum is observed at MgO; the value for

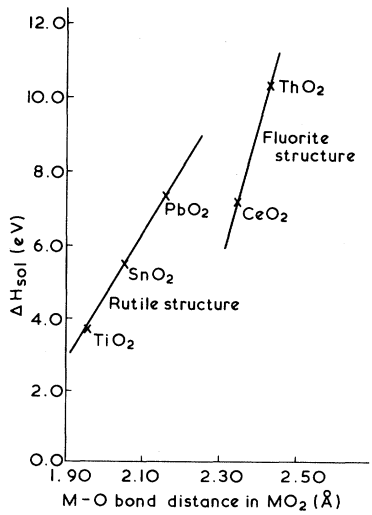

FIG. 1. Calculated heats of solution for oxides of divalent metal ions in Al_2O_3 host.

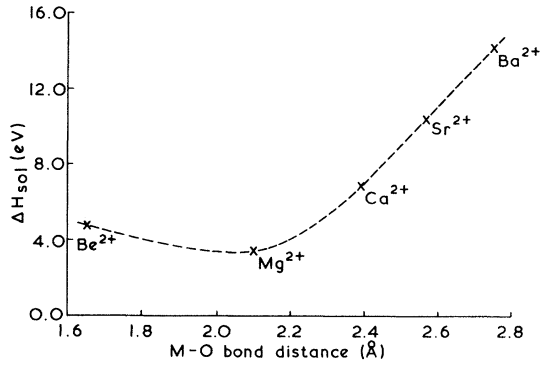

FIg. 2. Calculated heats of solution for oxides of tetravalent ions in Al_2O_3 host.

BeO is higher due to the exceptionally large lattice energy of the latter oxide.

Finally we note from Table VII that our predicted heats of solution for MgO in Al_2O_3 is in good agreement with the data of Roy and Coble.[35] This provides a valuable confirmation of the validity of our host lattice potentials. Investigations of the solution of dopants into Al_2O_3 may, however, be complicated by the possibility of accompanying redox reactions; these will be discussed in the following section.

3. *Dopant solution with oxygen loss or gain from the host lattice*

Before examining the redox reactions which may accompany doping of Al_2O_3, we discuss briefly the oxidation and reduction of the pure oxide. Oxidation with the formation of holes (assumed to be small polarons) may occur either by cation vacancy or interstitial formation, i.e., we have two possible reactions. First,

$$O_2(g)+\tfrac{4}{3}Al_{Al}^{3+}\rightarrow\tfrac{4}{3}V_{Al}+4h+\tfrac{2}{3}Al_2O_3$$

(where Al_{Al}^{3+} is a lattice aluminum ion, V_{Al} is an aluminum vacancy, h is a hole, and Al_2O_3 is aluminum on the surface of the oxide), and second,

$$O_2(g)\rightarrow 2O_i^{2-}+4h$$

(where by O_I^{2-} we indicate an oxygen interstitial). High values of 25.98 and 41.91 eV are calculated using nonempirical potentials for the vacancy and interstitial reactions, respectively.

When we consider reduction, there are again two possibilities. First, there is oxygen loss by vacancy creation, involving the reaction

$$2O_O^{2-}\rightarrow O_2(g)+2V_O+4e_c$$

(where O_O^{2-} is a lattice oxygen ion, V_O is a vacancy, and e_c is a conduction-band electron). Alternatively, interstitials could be formed when oxygen is lost, i.e., by the reaction

$$2O_O^{2-}+\tfrac{4}{3}Al_{Al}^{3+}\rightarrow O_2(g)+\tfrac{4}{3}Al_I^{3+}+4e_c$$

(where Al_I^{3+} is an interstitial). Again we find high heats of reduction of 17.95 and 19.71 eV for vacancy and interstitial modes, respectively.

From the magnitudes of these values we conclude that pure Al_2O_3 would show negligible deviations from stoichiometry—a result which is in accord with observations on the purest experimental materials. We now continue with our account of redox reactions in tetravalent and divalent doped crystals.

a. Tetravalent ions

When tetravalent ions enter the Al_2O_3 host, oxygen may be lost with the consequent release of electrons. These now compensate the effective charge of the dopant. If we assume that vacancies are the favored lattice-defect compensators, then the vacancy population will be in equilibrium with gaseous oxygen and electrons. As we shall show, the final state of these electrons is the controlling factor in determining the ease of oxygen loss. Let us first consider the possibility that electrons are released to the conduction band. For the vacancy and electron modes of compensation we have

$$3TiO_2+4Al_{Al}^{3+}\rightleftarrows 2Al_2O_3+3Ti_{Al}^{4+}+V_{Al}$$

and

$$4TiO_2+4Al_{Al}^{3+}\rightleftarrows 2Al_2O_3+4Ti_{Al}^{4+}+4e_c+O_2(g)\,,$$

in which e_c denotes an electron in the conduction band. From these two processes we derive the equilibrium equation

$$\tfrac{2}{3}Al_2O_3+\tfrac{4}{3}V_{Al}\rightleftarrows O_2(g)+4e_c+\tfrac{4}{3}Al_{Al}^{3+}\,.$$

(The mechanism of vacancy annihilation by oxygen loss presumably involves cation vacancy migration to the surface; the oxygen vacancies left by the oxygen released to the gas phase and the cation vacancies are mutually annihilated at the surface.)

The energy E_{O_2} of this process per eliminated oxygen molecule is given by

$$E(O_2) = -\tfrac{4}{3}E(V_{Al}) - \tfrac{2}{3}E(Al_2O_3) + 4E(e_c) + E_{12}^0 - D(O_2)\,, \quad (5.10)$$

where $E(e_c)$ is the energy of the conduction-band electron, E_{12}^0 is the sum of the first and second electron affinities of oxygen, and $D(O_2)$ the dissociation energy of oxygen. The component energies and resulting value of $E(O_2)$ are given in Table VIII. The value of 0.82 eV for $E(O_2)$ suggests that titanium-doped alumina could release oxygen by this mechanism. Furthermore, if we allow for the trapping of the electron by Ti^{4+} ions to form Ti^{3+}, then the release of oxygen is described by

$$6Ti_{Al}^{4+} + 2V_{Al} + Al_2O_3 \rightleftarrows \tfrac{3}{2}O_2(g) + 6Ti_{Al}^{3+} + 2Al_{Al}^{3+}$$

for which the energy per eliminated oxygen molecule is now -10.02 eV. At infinite dilution, then, our calculations suggest that the doping of Al_2O_3 by Ti^{4+} could lead to the release of oxygen and the possible reduction of the dopant to Ti^{3+}. The problem could, however, be complicated by two factors. First we have assumed that complete thermodynamic equilibrium can be maintained between the gas phase and the crystal. This may not be possible if the aluminum vacancy mobility is low, in which case oxygen loss may take place with anion vacancy formation rather than cation vacancy annihilation, for which the calculated value of $E(O_2)$ is 5.57 eV—a value which would lead to negligible oxygen loss. The second factor which may render oxygen loss less favorable is clustering between the vacancy and the Ti^{4+} dopant—a point to which we return later.

b. Divalent ions

Here, oxygen *gain* may accompany dissolution of the dopant in the Al_2O_3 host, with consequent creation of holes in the valence band. These holes now compensate the effective charge of the dopant ion. Once more the possibility of redox reactions will lead to an equilibrium between the point-defect compensators discussed in Sec. IV and the hole population. Thus for the vacancy and hole compensation models, we have:

$$2MgO + 2Al_{Al}^{3+} + O_O^{2-} \rightleftarrows Al_2O_3 + 2Mg_{Al}^{2+} + V_O$$

and

$$4MgO + O_2 + 4Al_{Al}^{3+} \rightleftarrows 2Al_2O_3 + 4Mg_{Al}^{2+} + 4h$$

in which h denotes a valence-band hole. As before, from these processes we derive the equilibrium equation

$$O_2(g) + 2V_O \rightleftarrows 4h + 2O_O^{2-}\,.$$

The energy $E(O_2)$ of the oxygen gain reaction for doped lattice is given by

TABLE VIII. Energies (eV) of redox reactions in doped Al_2O_3. (a) Component terms. (b) Energy of reduction of Ti^{4+}-doped Al_2O_3. (c) Energy of oxidation of Mg^{2+}-doped Al_2O_3.

(a) Component terms	
Conduction-band energy	-1.0
Hole-formation energy	7.7
Sum of O^{2-} and O^- ionization potentials in α-Al_2O_3[a]	-8.2
Dissociation energy of O_2	5.15
Cohesive energy of Al_2O_3	161.8
Cation vacancy formation energy	61.15
Anion vacancy formation energy	21.75
Fourth ionization potential of titanium[b]	42.81
(b) Energy of reduction of Ti^{4+}-doped Al_2O_3	
Conduction-band electrons	0.82
Ti^{3+}	-10.02
(c) Energy of oxidation of Mg^{2+}-doped Al_2O_3	8.85

[a]Effective ionization potential of O^- in α-Al_2O_3, -0.2 eV extrapolated from alkaline-earth oxide values (5).
[b]Reference 36.

$$E(O_2) = -2E(V_O) + 4E(h) - 2E^0_{12} + D(O_2) , \quad (5.11)$$

where $E(h)$ is the hole formation energy. Again we report component energies and the resulting value of $E(O_2)$ in Table VIII. With regard to our calculated value of $E(O_2)$, namely 8.85 eV, we stress that this is based on a *small-polaron* model for the free hole. However, as discussed by Colbourn and Mackrodt,[32] the large polaron could be more stable than the localized hole in which case our value for $E(O_2)$ will be reduced and could, in fact, be negative. Again we note that our calculations omit the effect of defect clustering; the inclusion of this factor has a significant effect on our predictions as will be seen in the next section.

B. Defect clustering: higher dopant concentrations

1. Clustering in absence of oxygen exchange with atmosphere

a. Tetravalent ions

We examine clustering of Ti^{4+} substitutionals with both cation vacancies and the alternative O^{2-} interstitial compensators; we recall that it was not possible to decide from our calculated defect energies which compensation mode would be favored. The most obvious dopant-interstitial cluster has two Ti^{4+} substitutionals at the nearest-neighbor (NN) site with respect to the interstitial. Thus the effective charge of O^{2-} interstitials is neutralized by the Ti^{4+} substitutional in adjacent sites along the c axis of the corundum structure. We find a high binding energy of 3.05 eV for this cluster.

We then examined substitutional-vacancy interactions. Again, a simple electroneutral cluster can be proposed in which three Ti^{4+} substitutionals are placed in the nearest-neighbor cation sites with respect to the cation vacancy. Once more, we find the cluster to be strongly bound; the calculated binding energy is 5.23 eV.

This result has three general consequences. The first follows from the magnitudes of the calculated binding energies. These are far larger than generally obtained in oxides—a consequence of the short interionic spacings and low dielectric constant of Al_2O_3. Cluster formation will dominate the defect structure of doped alumina at all but the lowest dopant concentrations. Thus a simple treatment using a mass-action formalism suggests that for Ti^{4+} concentrations of 1 ppm clustering will dominate at temperatures below 1500 K. The second point concerns the relative magnitudes of the interstitial and vacancy clustering energies. Although both are large, the binding of the vacancy with the substitutional is significantly greater. This factor strengthens the argument for vacancy rather than interstitial compensation in tetravalent doped materials. Third, we should note that clustering will have a major effect on defect formation energies deduced from measurements on doped crystals (see, e.g., the analysis of Mohapatra and Kroger[36]). The formation energies will in effect be reduced by the large stabilizing term provided by the interaction. We find that similar conclusions emerge from our analysis of clustering in the divalent-doped oxides which we present below.

2. Clustering in divalent-doped oxides

From our analysis of the defect structure of Mg^{2+}:Al_2O_3 at high dilution, substitutional vacancy and "self-compensation" emerged as the most probable mode of solution of such dopants. The simplest cluster based on the vacancy mode of compensation is that in which two substitutionals occupy nearest neighbor sites with respect to the vacancy. For the self-compensating mode, an equally simple model can be proposed: The charge at the Mg^{2+} interstitial is neutralized by two Mg^{2+} substitutionals situated above and below the interstitial site along the c axis. The calculated binding energies are presented in Table IX. Both clusters are strongly bound, but the binding energy of the vacancy-substitutional aggregate is significantly greater. Clustering will therefore strongly favor the vacancy mode of charge compensation. And, as with the Ti^{4+}-doped crystals, the magnitudes of the calculated binding energies suggest that cluster formation will dominate at all but the lowest dopant concentration, and that there will be a major effect on defect energies deduced from the analysis of doped crystals.

3. Clustering with electronic species

a. Tetravalent-doped crystals

We have shown in Sec. V A 3 that oxygen loss from crystals containing, e.g., Ti^{4+} results in the removal of point defects and the creation of elec-

TABLE IX. Cluster binding energies (eV). Figures in parentheses are the calculated heats of solution ΔH_{sol} in eV, allowing for clustering.

Cluster of two Ti^{4+} substitutionals with one oxygen interstitial	3.05(5.9)
Cluster of one cation vacancy and three Ti^{4+} substitutionals	5.23(1.79)
Cluster of two Mg^{2+} substitutionals and one anion vacancy	2.56(1.87)
Cluster of one Mg^{2+} interstitial with two Mg^{2+} substitutionals	2.43(2.22)

trons in the conduction band. The Ti^{4+} substitutional would, however, be expected to function as an ionized donor, i.e, there should be a significant trapping energy for electrons at the Ti^{4+} sites, effectively converting these into Ti^{3+} ions. We have estimated this energy by combining calculations of the lattice energy of the Ti^{4+} and Ti^{3+} substitutionals (which used potentials for the Ti^{4+}- and Ti^{3+}-lattice interactions obtained from the electron-gas procedures discussed in Sec. III) with the fourth ionization potential of Ti. The resulting trapping energy of 2.4 eV (Ref. 32) compares with a value of 2.77 eV deduced by Mohapatra and Kroger[36] from electrical conductivity measurements.

b. Divalent-doped crystals

Oxidation of, e.g., Mg^{2+}-doped Al_2O_3 results in hole formation. A simple cluster of one substitutional with one hole localized on the neighboring oxygen lattice site may form. If we assume that the hole is localized on the oxygen site nearest to the Mg^{2+} substitutional, we calculate a binding energy of 0.56 eV. A binding energy of this magnitude would be sufficient to lead to the majority of hole species being bound to the impurity at room temperature. We should note, however, that these models for the Mg^{2+}-hole clusters may be oversimplified, for Cox[37] has suggested that the preferred location of the hole is the further of the two sites. And indeed, recent work of Colbourn *et al.*[38] finds an increased binding energy of 0.7 eV for this complex. Mohapatra and Kroger[39] report a value of 1.95 eV for the binding energy, but Cox[40] has recently obtained a value of 0.7 eV from recombination kinetics following uv excitation.

C. Electronic structure of doped Al_2O_3

Our conclusions as to the electronic structure of doped Al_2O_3 can be summarized as follows. We find that introduction of Ti^{3+} leads to donor centers with thermal ionization energies of 2.4 eV; Mg^{2+} results in acceptor levels with an ionization energy of 0.56 eV. Further details of impurity levels in Al_2O_3 are planned to be reported separately.[41]

VI. COMPARISON WITH EXPERIMENT

We turn now to a comparison of our results with the available experimental data. It is our intention to discuss the effect of these on transport properties[42] and the energy levels of impurities[41] in separate publications. Here we concentrate on energies of defect formation and oxidation and reduction, and in particular we compare our results with the data reported recently by Kroger and his coworkers.[33,36,39,43–45]

In terms of the basic defect structure two points emerge from our calculations: The first is the absolute magnitude of the defect energies, which determines the extent of the disorder; the second is the relative values of the defect energies for the various type of defect. With regard to the former, the values derived from empirical potentials are appreciably lower than those from electron-gas potentials, both ours and those reported by Dienes *et al.*[15] We have no definite knowledge at present as to which set of results is more reliable, though as we show later experiment favors the nonempirical results. With regard to the second point, namely the relative energies of the type of defect, we find the following order for the various types of po-

tential.
For the empirical potential:

$$E_{OF} < E_{Sch} < E_{AlF} .$$

For the electron-gas potential:

$$E_{Sch} < E_{AlF} < E_{OF} .$$

From Dienes *et al.*[15]:

$$E_{Sch} < E_{OF} < E_{AlF} .$$

In a recent examination of the thermodynamic data Mohapatra and Kroger[43] suggest that Schottky disorder is dominant in Al_2O_3 and derive an enthalpy per defect of 3.83 eV. This is somewhat lower than our calculated values of 4.70 and 5.14 eV, though as we have mentioned, estimates of the effective defect formation energies could be reduced when the influence of clustering is taken into account. Mohapatra and Kroger[43] also report a value of 4.45 eV for cation Frenkel defects, which is appreciably lower than our theoretical values (6.47 and 7.09 eV) and that found by Dienes *et al.*[15] (10.0 eV). Now a possible explanation for this discrepancy is that the theoretical values for the energy of a cation interstitial, Al_I^{3+}, are simply too high, thereby overestimating the Frenkel energy. This could certainly be the case, for there are inaccuracies in all calculations of this type, although the magnitude of the discrepancy is much larger than that found for other systems.[3,4] However, from a comparison of the enthalpies of oxidation discussed in detail below, we suggest that an alternative explanation is that the experimental values reported by Mohapatra and Kroger[43] are, in fact, too low. In particular, we suggest that the discrepancy between theory and experiment is attributable principally to the enthalpy of the oxidation reaction

$$\tfrac{3}{4}O_2(g) + 3e \rightleftarrows \tfrac{3}{2}O_O^{2-} + V_{Al}$$

used by Mohapatra and Kroger[43] to derive their Schottky and Frenkel formation energies. The present calculation suggests that their energy (enthalpy) for the above reaction might be seriously in error and that a value nearer the theoretical energy reported here would increase their formation energies for both Schottky and Frenkel defects to something approaching the theoretical estimates of both Dienes *et al.*[15] and the present work.

Turning now to the oxidation of α-Al_2O_3 there are a number of processes by which this can take place. Of these, Kroger and co-workers have reported enthalpies for three:

$$\tfrac{1}{2}O_2(g) + V_O \rightleftarrows O_O^{2-} + 2h ,$$

$$\tfrac{3}{4}O_2(g) + Al_I^{3+} \rightleftarrows \tfrac{1}{2}Al_2O_3 + 3h ,$$

and that mentioned previously, namely,

$$\tfrac{3}{4}O_2(g) + 3e \rightleftarrows \tfrac{3}{2}O_O^{2-} + V_{Al} .$$

For the first of these we calculate an energy of 4.43 eV, i.e., half the value for Eq. (5.11), based on a small-polaron model for the hole, which agrees extremely well with the value of 4.05 eV reported by Mohapatra, Tiku, and Kroger.[44] If we used a large-polaron model[32] our calculated energy would be about 3.6 eV. For the second reaction we find an energy of 5.34 eV, which is slightly lower than, though still in good agreement with, the value of 6.57 eV derived by Dutt and Kroger.[45] The agreement with experiment for these two reactions lends support to the view that our energies for Al_I^{3+} are not grossly overestimated. For the last of the three reactions, however, we find considerable disagreement. Whereas we calculate an energy of -0.59 eV, Mohapatra and Kroger[43] report a value of -15.39 eV and it is this that is used to derive the Schottky and Frenkel defect energies. In arriving at our value of -0.59 eV we use three theoretically determined quantities, namely, the cation vacancy energy, the lattice energy of α-Al_2O_3, and the "effective" electron affinities of lattice oxygen. Our calculated lattice energy of -161.8 eV is 1.4 eV *lower* than that reported by Samsonov[23] so that our cation vacancy energy and electron affinity between them would have to be in error by about 15 eV, which seems unlikely in view of the good agreement we find for the first two reactions. We suspect, therefore, that the value reported by Mohapatra and Kroger[43] is substantially inaccurate, and in particular point to their value for $K_{ox,v}^{Ti}$ [Eq. (2.1) of Ref. 43] as being the possible source of error. Given this possibility, if we then assume a value of, say, -1.5 eV for the last of the three oxidation reactions, the Schottky energy per defect reported by Mohapatra and Kroger[43] would be increased by 2.8 to 6 eV and the cation Frenkel energy per defect by 7.0 to about 11.5 eV. Not only are these closer to the theoretical (nonempirical) energies, but they support the predominance of vacancy disorder even more strongly. Our results for transport properties and energy levels of impurities lend further support not only to this view but also to the greater reliability of the electron-gas potentials for α-Al_2O_3.

VII. CONCLUSIONS

This paper has concentrated first on questions of technique in the calculation of defect energies for noncubic oxides. Here we have shown that when dielectric anisotropy is appreciable, an adaptation of the Mott-Littleton method to allow of this anisotropy is essential. Regarding the effect on defect energies of lattice potentials, we find here that although a fair measure of agreement can be achieved between the result of empirical and nonempirical potentials for a large number of defects, in certain cases the nature of potential parameters can be critical. Thus the oxygen interstitial energy in Al_2O_3 is clearly highly sensitive to the potential. We suspect that this may be a general problem with interstitial energies in lattices with close packed anion sublattices. Limited comparison between theory and experiment has been possible, although further work is necessary in both areas. The present calculations provide, however, the first stage in advancing our detailed understanding of the defect properties of noncubic oxides.

ACKNOWLEDGMENTS

We are very grateful to Dr. M. J. Norgett for his valuable advice and assistance, and we wish to acknowledge his contribution to the program development reported in this paper. We are also indebted for useful discussions to Dr. L. W. Hobbs, Dr. A. H. Heuer, and Dr. A. M. Stoneham.

[1]C. R. A. Catlow, Proc. R. Soc. London Ser. A 353, 533 (1977).
[2]C. R. A. Catlow, W. C. Mackrodt, M. J. Norgett, and A. M. Stoneham, Philos. Mag. 35, 177 (1977); 40, 161 (1979).
[3]W. C. Mackrodt and R. F. Stewart, J. Phys. C 12, 431 (1979).
[4]W. C. Mackrodt and R. F. Stewart, J. Phys. C 12, 5015 (1979).
[5]N. F. Mott and M. J. Littleton, Trans. Faraday Soc. 34, 485 (1938).
[6]C. R. A. Catlow and B. E. F. Fender, J. Phys. C 8, 3267 (1975).
[7]C. R. A. Catlow and R. James (unpublished).
[8]A. B. Lidiard and M. J. Norgett, in *Computational Solid State Physics,* edited by F. Herman, N. W. Dalton, and T. R. Koehler (Plenum, New York, 1972).
[9]M. J. Norgett, AERE (Atomic Energy Research Establishment) Report No. AERE-R7015 (unpublished).
[10]M. J. Norgett, AERE Report No. AERE-R7605 (unpublished).
[11]P. T. Wedepohl, Proc. Phys. Soc. London 92, 79 (1967); J. Phys. B 1, 307 (1968); J. Phys. C 10, 1855 (1977); 10, 1865 (1977).
[12]R. G. Gordon and Y. S. Kim, J. Chem. Phys. 56, 3122 (1972).
[13]Y. S. Kim and R. G. Gordon, J. Chem. Phys. 60, 1842 (1974); 60, 4332 (1974); Phys. Rev. B 9, 3548 (1974).
[14]C. R. A. Catlow and M. J. Norgett, J. Phys. C 6, 1325 (1973).
[15]G. J. Dienes, D. O. Welch, C. R. Fischer, R. D. Hatcher, O. Lazareth, and M. Samberg, Phys. Rev. B 11, 3060 (1975).
[16]M. J. Norgett and R. Fletcher, J. Phys. C 3, L190 (1970).
[17]R. Fletcher and M. D. J. Powell, Computer J. 6, 163 (1963).
[18]W. C. Mackrodt, J. Comp. Phys. (in press).
[19]B. G. Dick and A. W. Overhauser, Phys. Rev. 112, 90 (1958).
[20]C. R. A. Catlow, D. Phil. Thesis, University of Oxford, 1974 (unpublished).
[21]C. R. A. Catlow, R. James, and M. J. Norgett, J. Phys. (Paris) Colloq. C7, 443 (1976).
[22]C. R. A. Catlow and R. James, J. Phys. C. 10, L237 (1977).
[23]G. V. Samsonov, *The Oxide Handbook* (IFI/Plenum, New York, 1973).
[24]J. B. Wachtman, W. E. Tefft, D. G. Lam, and R. B. Stinchfield, J. Res. Nat. Bur. Stand., 64A, 213 (1960).
[25]K. F. Young and H. P. R. Frederikse, J. Phys. Chem. Ref. Data 2, 313 (1973).
[26]B. F. Levine, Phys. Rev. B 7, 2591 (1973).
[27]J. G. Traylor, H. G. Smith, R. M. Nicklow, and M. K. Wilkinson, Phys. Rev. B 3, 3457 (1971).
[28]S. C. Keeton and W. D. Wilson, Phys. Rev. B 7, 834 (1973).
[29]A. I. M. Rae, Chem. Phys. Lett. 18, 574 (1973).
[30]A. M. Stoneham, AERE Report No. R9598 (unpublished).
[31]I. D. Faux and A. B. Lidiard, Z. Naturforsch. 26a, 62 (1971).
[32]E. A. Colbourn and W. C. Mackrodt, Solid State Commun. (in press).
[33]W. H. Strehlow and E. L. Cook, J. Phys. Chem. Ref. Data 2, 163 (1973).
[34]C. R. Viswanathan and R. Y. Loo, Appl. Phys. Lett. 21, 370 (1972).
[35]S. K. Roy and R. L. Coble, J. Am. Ceram. Soc. 51, 1 (1968).
[36]S. K. Mohapatra and F. A. Kroger, J. Am. Ceram.

Soc. 60, 381 (1977).
[37]R. T. Cox, These, L'Universite Scientifique et Medicale de Grenoble, 1972 (unpublished).
[38]E. A Colbourn, W. C. Mackrodt and W. E. Smith (unpublished).
[39]S. K. Mohapatra and F. A. Kroger, J. Am. Ceram. Soc. 60, 141 (1977).
[40]R. T. Cox, Proceedings of the 1st Annual Conference, European Physical Society (Condensed Matter Division), Antwerp, 1980.
[41]E. A. Colbourn, J. Kendrick and W. C. Mackrodt (unpublished).
[42]C. R. A. Catlow, E. A. Colbourn, R. James, and W. C. Mackrodt (unpublished).
[43]S. K. Mohapatra and F. A. Kroger, J. Am. Ceram. Soc. 61, 106 (1978).
[44]S. K. Mohapatra, S. K. Tiku, and F. A. Kroger, J. Am. Ceram. Soc. 62, 50 (1979).
[45]B. V. Dutt and F. A. Kroger, J. Am. Ceram. Soc. 58, 474, (1975).
[46]R. W. G. Wyckoff, *Crystal Structures,* Vol. 1 (Interscience, New York, 1963); Vol. 2 (1964), Vol. 3 (1965).
[47]M. J. Norgett, A. M. Stoneham, and A. P. Pathak, J. Phys. C 10, 555 (1977).